A channelopathy mechanism revealed by direct calmodulin activation of TrpV4

Stephen H. Loukin[a,1], Jinfeng Teng[a], and Ching Kung[a,b,1]

[a]Laboratory of Molecular Biology, University of Wisconsin, Madison, WI 53706; and [b]Department of Genetics, University of Wisconsin, Madison, WI 53706

Ca^{2+}-calmodulin (CaM) regulates varieties of ion channels, including Transient Receptor Potential vanilloid subtype 4 (TrpV4). It has previously been proposed that internal Ca^{2+} increases TrpV4 activity through Ca^{2+}-CaM binding to a C-terminal Ca^{2+}-CaM binding domain (CBD). We confirmed this model by directly presenting Ca^{2+}-CaM protein to membrane patches excised from TrpV4-expressing oocytes. Over 50 *TRPV4* mutations are now known to cause heritable skeletal dysplasia (SD) and other diseases in human. We have previously examined 14 SD alleles and found them to all have gain-of-function effects, with the gain of constitutive open probability paralleling disease severity. Among the 14 SD alleles examined, E797K and P799L are located immediate upstream of the CBD. They not only have increase basal activity, but, unlike the wild-type or other SD-mutant channels examined, they were greatly reduced in their response to Ca^{2+}-CaM. Deleting a 10-residue upstream peptide (Δ795–804) that covers the two SD mutant sites resulted in strong constitutive activity and the complete lack of Ca^{2+}-CaM response. We propose that the region immediately upstream of CBD is an autoinhibitory domain that maintains the closed state through electrostatic interactions, and adjacent detachable Ca^{2+}-CaM binding to CBD sterically interferes with this autoinhibition. This work further supports the notion that TrpV4 mutations cause SD by constitutive leakage. However, the closed conformation is likely destabilized by various mutations by different mechanisms, including the permanent removal of an autoinhibition documented here.

skeletal dysplasia | calcium | ion channel | autoinhibition | TrpV1

Transient Receptor Potential (TRP) channels are a diverse family of cation-nonselective Ca^{2+}-permeable channels with only limited sequence homology. They are tetramers of subunits that have the 6-TM membrane topology common to cation channels. TRPs tend to be polymodal, activated by a wide variety of chemical and physical stimuli. TrpV4 (vanilloid subfamily, type 4), cloned on the bases of its response to hypotonicity, can also be activated by direct membrane stretch, mild heat, and by endogenous metabolites as well as synthetic chemicals (1–3). The most potent agonist, GSK1016790A (abbreviated as GSK herein) (4) can drive the TrpV4 open probability (Po) to almost 100% (5).

Ca^{2+} regulations of TRP channels are varied and complex. They often show Ca^{2+}-dependent desensitizations to various stimuli by multiple mechanisms including the action of Ca^{2+}-calmodulin (6, 7). In the case of TrpV4, however, Ca^{2+} increases (potentiates) channel response to hypotonicity or to phorbol esters (4αPDD or 4αPMA), although the activated current is followed by a Ca^{2+}-dependent inactivation (8, 9). Strotmann et al. (9) found that the potentiation by Ca^{2+} requires an intact calmodulin (CaM) binding site (CBD) within Q806–E831 in the C-terminal tail. They later proposed that, without Ca^{2+}-CaM, the CBD docks on an N-terminal site causing closure (10).

At least 57 mutations in *TRPV4* have been found to underlie dominantly heritable forms of skeletal dysplasia (SD) with several clinically distinguishable presentations, adult neuro-muscular degenerations, as well as being associated with other genetic predispositions. See ref. 3 for a review. We have shown that of 14

representative SD-causing *TRPV4* alleles all encode channels with increased constitutive Po when expressed in *Xenopus* oocytes and that the level of basal leakage correlated with the clinical severity of the SD they caused (5). We therefore believe that SD mutations are likely all gain-of-function (GOF) alleles. None of the disease alleles falls within Q806–E831, the putative CBD. However, two GOFs we examined, E797K and P799L, are immediately upstream from this CBD (5). Fig. 5A diagrams this region of interest. E797K has been repeatedly discovered in different families (3, 11). P799 appears to be a hot spot with several known alleles: P799A, P799S, P799R, and the first-reported P799L (11, 12), causing different types of SD. Here, we scrutinized E797K, P799L, and several engineered mutations to further our understanding of TrpV4's Ca^{2+}-CaM regulation and its relationship to channelopathy.

To avoid the complexity of the cytoplasm in whole cells, we here directly present CaM protein to membrane patches excised from *TRPV4*-expressing oocytes. Channel activation by such presentation was first demonstrated with patches excised from *Paramecium* (13). Rosenbaum et al. (6) showed that direct application of Ca^{2+}-CaM reduces capsaicin-activated current of TrpV1 in expressing oocyte patches. Thus, CaM can be regarded as a detachable channel subunit in these cases. We found Ca^{2+}-CaM alone robustly activates wild-type TrpV4 current in the absence of added chemical or physical stimuli such as GSK or stretch force, and therefore refer to the effect as activation instead of potentiation. We found that E797K and P799L channels are uniquely defective in activation by Ca^{2+}-CaM. Further investigation led us to postulate that the peptide at the I795-I804 region, which covers these mutations, likely binds to other gating elements to stabilize the closed state(s) and that Ca^{2+}-CaM release the binding to open TrpV4. This is akin to the classical disinhibition mechanism

Significance

Over 50 mutations in the ion channel Transient Receptor Potential vanilloid subtype 4 (TrpV4) cause diseases ranging from dwarfism to prenatal death. We previously examined 14 mutant channels and found them to leak. Ca^{2+} encourages TrpV4 opening through calmodulin (CaM). Here, we examined two channels mutated in close proximity to the Ca^{2+}-CaM–binding domain. They not only leak but also are greatly reduced in activation by Ca^{2+}-CaM compared with the wild-type or other mutant channels. These mutations likely define an autoinhibitory domain that keeps the channel closed, to which adjacent detachable Ca^{2+}-CaM binding interferes with this inhibition. The scattered disease alleles may all make the channel leak but apparently by different means, including the loss of an autoinhibition shown here.

of enzyme activation, in which an autoinhibitory peptide is removed by Ca^{2+}-CaM to activate.

Results

The central experiments in this work entail the activation of TrpV4 in hundreds of excised patches by Ca^{2+}-CaM. There was large variability in this response. Wild-type channels ranged from no response in about 20% of the patches to <10-fold to >500-fold in those that did respond. We attribute this variability to access resistance to CaM protein by underlying membrane debris, and underscore the challenge of such direct, but rarely performed experiments. Such variability makes comprehensive statistical analysis misleading, because it reflects mostly variability in access resistance, not CaM activation. Conclusions are instead drawn from observing changes in channel opening probabilities (Po) within individual patches in response to stimuli, observed repeatedly in multiple independent patches. Key observations are illustrated with exemplar patches (Figs. 1–3 and Figs. S1–S4) and ranges of variations among patches are given in the text. To facilitate the observations of Po changes in patches, expression levels were set and exemplar traces were chosen so that appropriate unitary channel activity could be observed throughout the experiment (see Fig. 1 legend and *Methods* for further clarification).

Direct Activation of TrpV4 by Exogenously Added Ca^{2+}-Calmodulin. The model of Strotmann et al. (9) was supported by whole-cell recordings from expressing HEK293 cells treated with hypotonicity or 4αPMA. To avoid the complications of added stimuli and the complexity of the cytoplasm, we have chosen to present Ca^{2+}-CaM directly to TrpV4 channels in inside-out patches excised from expressing *Xenopus* oocytes. Such experiments gave results that were more easily interpreted but were technically challenging, requiring modifications of the methods used previously (5, 14) (*Methods*). Fig. 1A illustrates a typical strong activation by Ca^{2+}-CaM. Before reaching maximal expression at 4 d after cRNA injection (*Methods*), wild-type TrpV4 had a very low spontaneous open probability (Po) (region "i" in the continuous trace and all point histogram below) in the absence of stimuli. Addition of 1 μM bovine CaM to the bath (with 100 μM Ca^{2+}) dramatically increased Po (region "ii"). This exogenous CaM activation was Ca^{2+}-dependent, as chelation of Ca^{2+} by addition of 0.5 mM BAPTA eliminated (region "iii") and subsequent further addition of 1 mM Ca^{2+} restored ("iv") activity. All-point histograms document the Po increase (ii and iv) and indicate a unitary conductance of ~80 pS expected of TrpV4 in

the ionic conditions used. Ca^{2+}-CaM activation was variable among the >100 patches examined, yielding no detectable Po increase in ~20% of cases to robust activations of 115 ± 34 fold (sem, n = 21). A key observation by Strotmann et al. (9) was that the mutation W822A in the middle of the proposed Ca^{2+}-CaM–binding domain (CBD) (Fig. 5A) eliminated binding and removed potentiation. Indeed we found that in all of the >50 patches examined, presenting Ca^{2+}-CaM to patches expressing TrpV4 with an engineered W822A mutation showed no discernible significant increase in the Po (Fig. 1B). Note that in most cases a significant rundown of TrpV4 activity was observed within the first several seconds after patch excision, but in some cases such as can be seen in Fig. 1A (and even more notably in Fig. 3C below) extends throughout the experiment. It could clearly be recognized as rundown because it occurred throughout the recording and does not alter the salient qualitative conclusions as to whether or not channels are activated by Ca^{2+}-CaM. Because these experiments were carried out in the absences of added stimuli, we therefore refer to the Po increase as "activation" instead of "potentiation."

We have previously shown that the wild-type TrpV4 and a SD-causing mutant channel could both be directly activated by stretching the excised patches through pipet suctions (14). To ascertain whether W822A channels were specifically defective in their Ca^{2+}-CaM activation or were generally defective, we assessed their mechanosensitivity. Patch-to-patch variations notwithstanding, robust TrpV4 mechanosensitivity could be readily observed although the technical modifications that optimize Ca^{2+}-CaM presentation apparently compromised force delivery (*Methods*). Fig. 2A illustrates the robust and repeatable intrinsic mechanosensitivity often, but not always, observed of wild-type TrpV4 here. That this force-sensitive activity was due to ~80 pS TrpV4 is shown in the all-points histograms (Fig. 2B). W822A channels also displayed robust intrinsic mechanosensitivity (Fig. 2 C and D), confirming that its defect is specifically in its responding to Ca^{2+}-CaM and not a general gating failure.

Channels with Disease-Causing Mutations Near the CaM-Binding Site Are Constitutively Active and Defective in Activation by Ca^{2+}-CaM. We have previously examined 14 skeletal-dysplasias (SD)-causing channels and found them all have increased basal Po (5). Although no disease alleles have been reported in the CBD itself, E797K and P799X immediately upstream of this CBD (Fig. 5A) cause SD. Consistent with previous results from whole-cell recordings, both P799L and E797K in patches had higher basal activities than wild-type channels such that expression

Fig. 1. Exogenous Ca^{2+}-CaM activates wild-type TrpV4 but not TrpV4 with a key mutation that prevents Ca^{2+}-CaM binding. (A) A representative patch of low activity from oocytes expressing wild-type *TRPV4* was excised and clamped at a test potential of 80 mV in ionically symmetric solutions containing 0.1 mM $CaCl_2$ *Methods*). Little activity was observed at the start (region "i" in trace and all-points histogram below). At the point indicated in this continuous recording, 1μM bovine CaM was added to and mixed in the bath (mixing artifacts are shown, but grayed out in this and all subsequent traces) resulting in a substantial increase in TrpV4 activity ("ii"). Chelation of Ca^{2+} with 0.5 mM K^+ BAPTA suppressed (iii) and readdition of 1 mM $CaCl_2$ ("iv") restored this Ca^{2+}-CaM-dependent activation of the wild-type TrpV4. Zero current levels are indicated by

horizontal carats at left of traces. (B) Ca^{2+}-CaM presentation as in (A) to a representative patch with higher basal activity excised from an oocyte expressing the CaM-nonbinding W822A TrpV4 (9). No CaM activation can be discerned. Note that the initial basal Pos for the exemplar traces illustrated here were low for wild type, so that unitary activity could still be discerned after robust activation, yet higher for W822A, so that lack of activation could be demonstrated. We did not observe a systematically lower basal Po for W822A overall.
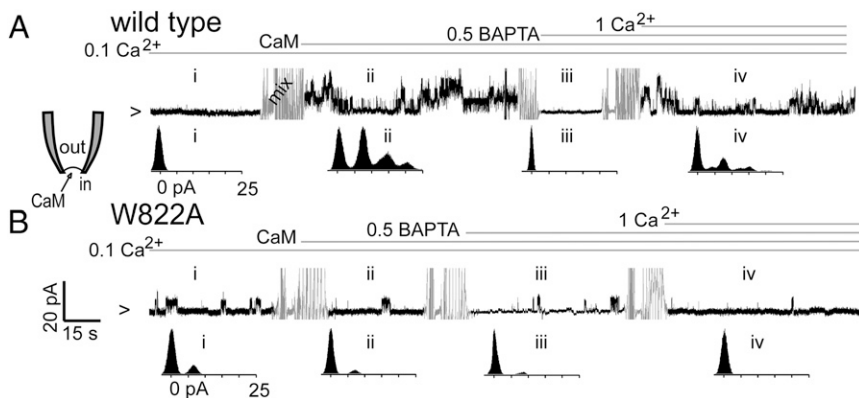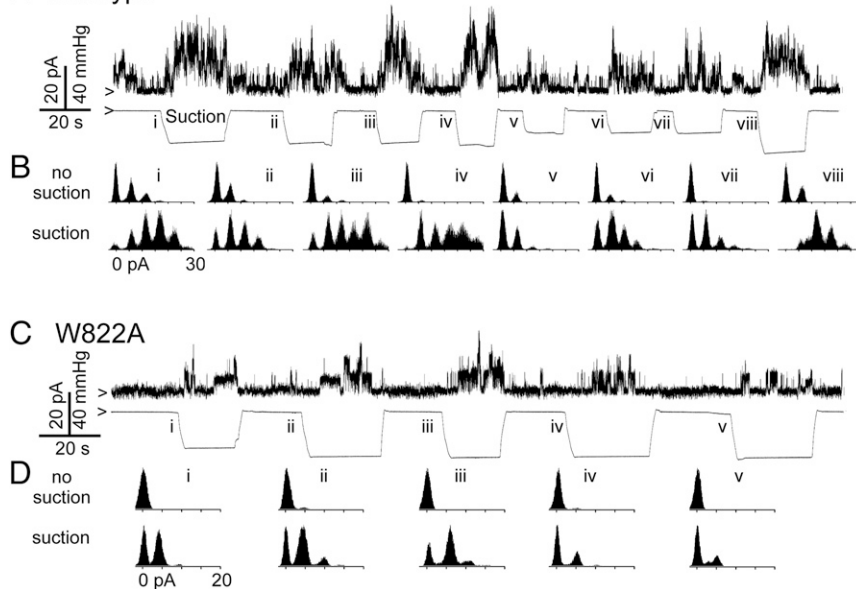
Fig. 2. W822A TrpV4 maintains activation by mechanical stimuli. (*A*) A continuous recording showing that the wild-type TrpV4 opened repeatedly in response to membrane stretch pulses in inside-out patches excised from oocytes. (*B*) All-point histograms corresponding to each regions from this trace before (*Upper*) and during suction (*Lower*). (*C* and *D*) A continuous recording showing that the CaM-nonresponding W822A TrpV4 channels maintain their mechanosensitivity. Recording conditions are identical to the initial conditions described in Fig. 1 and in *Methods* except that the test potential was 60 mV. Zero current/pressure levels are indicated by horizontal carats at the left in this and all subsequent figures.

levels had to be reduced to clearly observe single channel activity (Fig. 3 *A–D*, see *Methods*). In the majority of cases, addition of Ca^{2+}-CaM failed to activate P799L (Fig. 3 *A* and *B*, $n = 36$) or E797K (Fig. 3 *C* and *D*, $n = 20$). In some cases, however, mild activation could be detected (Fig. S1) with a 2.3 ± 0.3 fold

increase for P799L ($\pm$ SEM, $n = 14$) and a 2.4 ± 0.3 fold increase for E797K ($n = 16$) in these cases. That the lack of Ca^{2+}-CaM activation is not because of Po maximization and that the channels are not generally defective are shown by their ability to respond to mechanical force (Fig. 3 *E–H*).
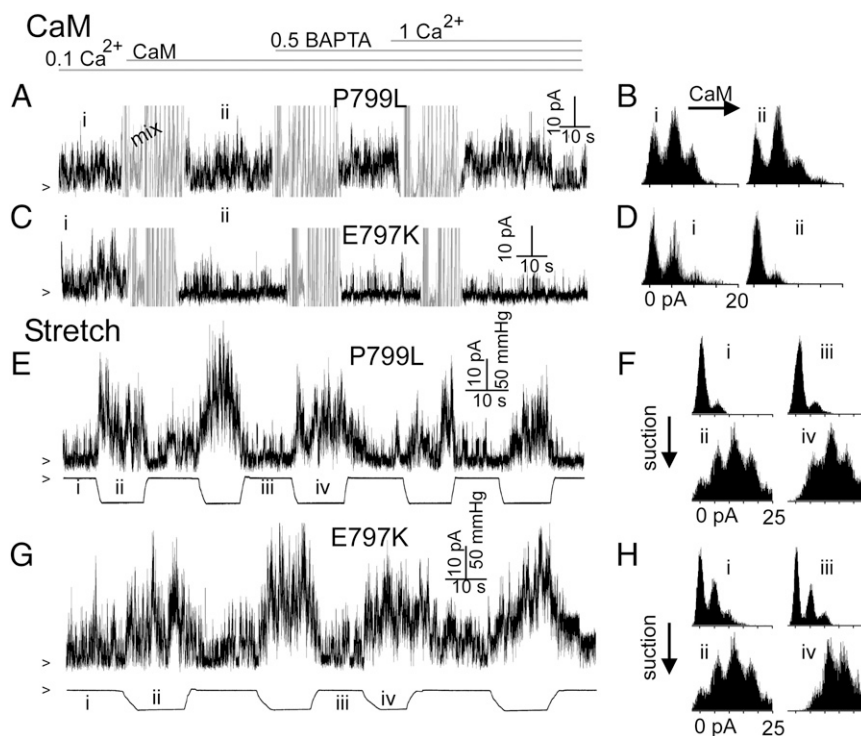

Fig. 3. TrpV4 with disease-causing mutations upstream of the CaM-binding domain resembles a constitutive Ca^{2+}-CaM activated state. (*A*) Oocytes expressing reduced levels of TrpV4 with P799L mutation, examined as in Fig 1 (except at a test potential of 60 mV) show strong constitutive activity, but in the majority of cases Ca^{2+}-CaM activation cannot be discerned (but see text and Fig. S1). (*B*) All-points histograms of the traces in *A* before (*i*) and after (*ii*) Ca^{2+}-CaM addition. *C* and *D* are arranged as *A* and *B* for the same examination of TrpV4 with the E797K mutation. Continuous recording from P799L (*E* and *F*) and E797K channels (*G* and *H*) showed that they were not generally defective in opening, being repeatedly activatable by membrane stretches. All point histograms on the right (*F* and *H*) correspond to the labeled regions in the traces with suction being present in the lower but not the upper two histograms in each case.

We also checked Ca^{2+}-CaM activation of SD-causing mutants not in close proximity to the CBD. Like wild type and unlike E797K/P799L channels, robust CaM activation of these mutants was readily observed in the majority of cases. V620I, predicted to be on the cytoplasmic end of S6, was readily activated by Ca^{2+}-CaM (Fig. S2A). Likewise T89I near the N terminus; D333G and Δ333–7 both in the ankyrin repeats, as well as R616Q in the S4-5 linker were all robustly activated by CaM (Fig. S2B). The maximal Ca^{2+}-CaM activations observed of these channels is qualitatively much greater than the maximal activation observed for E797K or P799L (Fig. S2C) despite the fact that fewer "other" channels were analyzed. Thus, it appears that the inability to be activated by Ca^{2+}-CaM is limited to channels with mutations in the peptide immediately upstream of CBD among the alleles tested here.

The E797-P799 Region Forms an AID Favoring Channel Closure. Two possible mechanisms can explain the results above: (*i*) After Ca^{2+}-CaM binding to the CBD, the upstream E797–P799 domain reconfigures to increase the relative stability of the open state; the mutant domain assumes the reconfigured form even in the absence of Ca^{2+}-CaM binding. (*ii*) It functions as an inhibitory domain favoring channel closure and adjacent Ca^{2+}-CaM binding interferes with this function. To distinguish between the two, we constructed a 10-aa deletion, ΔI795–I804, that encompasses E797 and P799 reasoning that such a significant deletion would destroy function (Fig. 5A). We have previously found that GSK can drive TrpV4 Po to near 100% (5). Thus, the constitutive basal Po of a channel can be assessed by comparing the whole-cell current densities before and after GSK exposure. Basal-current increase by a GOF mutation raises the floor and leaves less room for GSK-driven increase (5). At an injection of ~0.1 ng cRNA, the wild-type basal current was barely detectable (Fig. 4A, "wt" left) compared with water injected oocytes ("water" left), allowing us to register the huge increase by GSK without saturating the capacity of our recording system ("wt" right). Assuming the GSK-maximized current as approximating Po = 1, the estimated basal Po of the wild type TrpV4 was just $0.34 \pm 0.09\%$ (SEM, $n = 7$) (Fig. 4B "wt"). The TrpV4 mutated in its CBD (W822A), which fail to be activated by Ca^{2+}-CaM (Fig. 1B), had a similar low basal Po ($0.23 \pm 0.05\%$, $n = 6$, Fig. 4B "W822A") as expected. Both E797K and P799L have much higher basal Pos of $19 \pm 5\%$ ($n = 7$) and $24 \pm 5\%$ ($n = 8$, Fig. 4 A and B, "E797K" and "P799L"). Note that this basal Po is higher than the basal Po often observed in patches (e.g., E797K in Fig. 3A) suggesting that cytoplasmic factors in intact cells favor channel opening, a conclusion further supported by channel rundown that is often observed in excised patches. Deleting 10 residues surrounding E797-P799 region results in an even stronger GOF phenotype with basal Po of $41 \pm 5\%$ ($n = 11$, Fig. 4 A and B, "Δ795-804"), consistent with some residual AID activity remaining in the point mutants. Reversal of both E797 and D798 to K similarly had such higher basal Po of $44 \pm 3\%$ ($n = 5$, Fig. 4B "797/8KK") indicating that the remaining negative charge in at least the case of the E797K mutant was responsible for the residual AID activity. We also assessed the ability of Ca^{2+}-CaM to activate Δ795–804, and failed to detect any discernible activation ($n = 8$, Fig. S3) as with the W822A mutant (Fig. 1B). This increase in basal Po by I795–I804 domain deletion makes mechanism I untenable, but is consistent with mechanism II where it functions as an autoinhibitory domain (AID), and that this function is largely absent in the E797K and P799L and completely eliminated in the Δ795–804 mutants.

The only substitution of E797 found to cause disease so far is a charge reversal to K (3, 11). This glutamic acid residue is immediately followed by another acidic residue, D798, indicating that AID function may require salt bridging with positively charged domains elsewhere. Strotmann et al. (10) proposed that
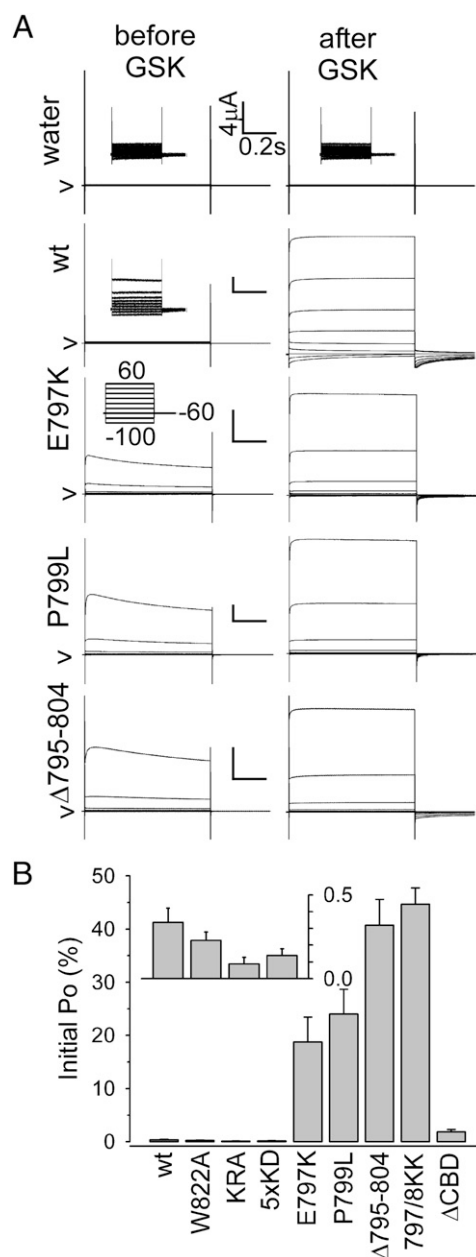

Fig. 4. Basal activity dramatically increased by deletion of the AID but not other key mutations. (*A*) Whole-oocyte currents were recorded with a two-electrode voltage clamp from oocytes injected with either water or a small amount (0.1 ng) of wild-type or mutant *TRPV4* cRNA. Only very low levels of TrpV4-specific basal current could be detected in wild-type injectants compared with water-injected oocytes (*Left*, inset traces have a 20-fold magnified current scale), whereas a dramatic increase in currents was observed after 5-min exposure to 1 μM GSK in the wild-type-*TRPV4* cRNA-injected but not the water-injected oocytes (*Right*). As we have shown (5), oocytes expressing *TRPV4-E797K* and -*P799L* have much higher basal current densities with relatively small increases after GSK exposure due to this (note that there was greater inactivation of these mutant currents here than previously observed, which we attribute to a change in our protocol designed to prevent inward Ba^{2+} flux through TrpV4, see *Methods*. TrpV4 with a 10-aa deletion (Δ795–804) removing the E797-P799 region, had high basal activity and likewise only nominal further stimulation by GSK. (*B*) Basal open probability (Po) estimated by the relative levels of leak-subtracted peak currents at 40 mV before and after GSK exposure from oocytes expressing the *TRPV4* alleles shown in *A*, and five more: the CaM-nonbinding W822A, the putative N-terminal binding domain mutants KRA and 5xKD (see text), the E77K/D798K double mutant and the CBD deletion mutant ΔCBD. (*Inset*) Pos of the low-basal Po mutants on an expanded *y* axis aligned to their identities on the main axis below (mean $\pm$ SEM, $n > 6$).

MEDICAL SCIENCES

a region containing a stretch of basic residues in the amino tail, RRK124-6, binds to the CBD to form a channel-closing auto-inhibitory complex that is dissociated by Ca^{2+}-CaM binding. Although that model has the RRK124-6 region binding the CBD itself when Ca^{2+}-CaM is not present, we entertained the possibility that salt bridging between the positively-charged basic residues of RRK124-6 and the negatively charged ED797-8 region, which precedes the CBD, may underlie an autoinhibition. The previous model was partly supported by showing a pre-potentiation by the "KRA" mutation, which substituted RRK124-6 with AAA124-6 (10). We found that, in whole oocytes, KRA has a very low Po similar to wild type (Fig. 4B, KRA). Likewise, the AAA124-6 substituted channels were readily activated by Ca^{2+}-CaM in excised patches (Fig. S4A). We found that even charge reversal of these residues as well as 2 near-adjacent basic residues ("5xKRD" KRWRRK121-6 to DDWDDD) similarly had a low basal Po ("5xKRD" in Fig. 4B) as well as robust CaM activation (Fig. S4B).

We also found that complete removal of the CaM binding domain, Δ809–831 ("Δ CDB", Fig. 4B), itself rich in basic residues, had relatively muted effects on basal current levels. Whereas deletion of the E797–P799 region caused a ~100-fold increase in basal Po, deletion of the CBD caused only an ~five-fold increase (Fig. 4B, "ΔCBD"). These observations further argue against the CBD itself being a primary component of any autoinhibitory complex.

In conclusion, it appears that the E797–P799 region is an AID. Mutation suggests that salt bridging is important for this function, but we have yet to identify a corresponding domain to which it binds to maintain closure. The recently solved molecular structure of TrpV1 hints at what the autoinhibitory interaction may be (Discussion).

Discussion

Ca^{2+}-CaM regulates a large number of channels by a variety of means (15, 16). Our model is akin to the classical activation mechanism whereby an autoinhibitory interaction is disrupted by the binding of diffusible Ca^{2+}-CaM to activate many enzymes (17, 18) and some channels (19, 20). This model is similar to that proposed by Strotmann et al. (10), where the CBD itself binds an N-terminal region (S117–S134) in the absence of CaM. They found that neutralizing three basic residues (124-126, RKK-to-AAA) left TrpV4 "permanently potentiated." Using our methods, we found that this "KRA" mutant was not permanently potentiated, having as low or even lower basal Po than wild type (Fig. 4B), and was readily activated by CaM when isolated in excised patches (Fig. S4). Even reversing all five basic residues in this region (R121D, RKK-to-DDD 124–6, K130-D) had no discernible effect (5xKRD, Fig. 4B and Fig. S4B). In addition, we found that removing the CBD itself only nominally increased basal Po (Fig. 4B). The discrepancy may reflect the vastly different experimental systems. Although likely not completely free of submembrane debris (Methods), our excised patches were essentially just TrpV4 in membrane responding instantly to experimental manipulations. Previous works were performed with whole HEK293 cells, with cytoplasmic metabolism largely intact. In those works, responses to agonists took tens of seconds and residual Ca^{2+} in nominal Ca^{2+}-free solutions was not chelated (10). Curiously, this same N-terminal region has subsequently been implicated in the binding to and potentiation of TrpV4 by PIP_2, which further complicate the chemistry in intact cells (21).

AID Model. The charge reversing nature of the E797K mutation and the adjacent D798 residue leads us to suspect that the AID salt bridges with another positively-charged domain promoting channel closure (note that a point mutation cannot reverse the charge of D798, explaining the lack of disease mutations there). The simplest scenario is that the negatively charged E797-D798 interacts with a positively charged region elsewhere, yet to be defined, preventing channel opening (Fig. S5A, state a). Our results ruled out the basic residues of the amino domain or those of the CBD itself being the partner. This inhibitory interaction apparently also requires a subsequent kink in the backbone structure as evidenced that P799L is also in a constitutively CaM-activated state (Fig. 3 A and B) and several other substitutions of this proline also cause disease (22). Fig. S5A illustrates the simplest (fewest state) model, where AID complex association and CaM binding are mutually exclusive. Spontaneous AID
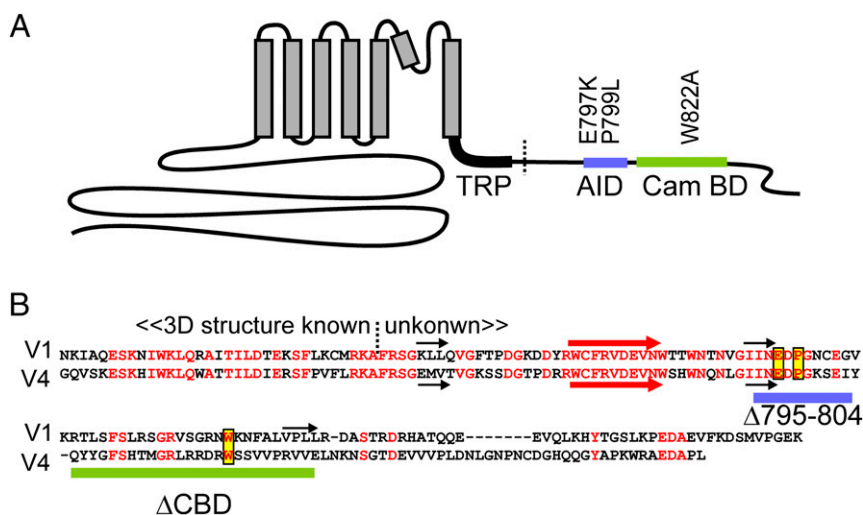

Fig. 5. Autoinhibitory and CaM-binding domains in carboxyl tail. (A) Topological cartoon illustrating key regions of the carboxyl domain of TrpV4 considered in this work including the CaM-binding domain (CBD, green) and the proposed AID (blue). Also shown are the locations of the human SD mutations E799K and P799L as well as the engineered CaM-binding mutation W822A. (B) Alignment of the entire carboxyl termini of TrpV1 (Upper) and V4 (Lower). Identical residues (red) indicated conservation through but not beyond the AID. The extent of the known cryo structure of TrpV1 is indicated by the vertical dotted line (in A as well). Extended β-sheet (arrows) secondary structures predicted using PSSpred (Y. Zhang, zhanglab.ccmb.med.umich.edu/PSSpred) are indicated above and below the primary sequences for TrpV1 and TrpV4, respectively, with the red arrow highlighting the likely undefined β sheet from the cryo structure. Point mutants examined in this study are indicated by yellow boxes, the blue bar indicates the extent of the AID deletant and the green to the CBD deletant.

complex dissociation is followed by CaM binding (states a to b to d) allowing channels to open (d to e). Deleting the AID strongly favor its dissociation (purple transitions in Fig. S5*A*) resulting in the majority of these channels residing in a closed but openable state (state b) even in the absence of CaM. Disease-causing point mutations also favor this dissociation, but not quite as strongly. In contrast other non-AID mutants have higher basal Pos due to increases in channel-opening equilibriums subsequent to AID dissociation (red transitions from a to b in Fig. S5*A*). Simplistic order-of-magnitude assumptions of these equilibriums can in fact predict that AID mutants having high basal Pos will have little further influence from Ca^{2+}-CaM binding, whereas non-AID-gating mutants having similarly high basal Pos will be very responsive to CaM (Fig. S5*B*). This analysis, although highly simplified, is consistent with our observations and supports the AID model.

TrpV1 and V4 share strong identity up to but not beyond the EDP residues of the AID (Fig. 5*B*). In both cases these regions are immediately followed by demonstrated CBDs with little primary homology, suggesting similar AID function in TrpV1. In the cryo-structure of TrpV1 an undefined beta sheet from the carboxyl tail forms the top of a tripartite antiparallel β sheet complex (23), which would orient residues immediately downstream of this β sheet toward the central axis of the cytoplasmic domains. Curiously, one of the best candidates for this β sheet in both TrpV1 and V4 is immediately upstream of the presumptive AID (Fig. 5*C*, red arrow), which would potentially orient it where it could easily form either intra- or intersubunit AID complexes to prevent channel opening. The most well characterized effect of Ca^{2+}-CaM on TrpV1 is desensitization (24), but this function is thought to primarily occur through binding to a lower-affinity site in the ARD of the N terminus (6, 25). Curiously, mutations which prevent CaM binding to this C-terminal CBD in fact have subdued peak current densities (ref. 26, figure 8C) and are more slowly activating (ref. 27, figure 3B), suggesting that the C-terminal site possibly serves potentiating role in V1 as well, the characterization of which could be masked by the more prominent desensitization under the experimental paradigms used to study TrpV1.

TRPV4 and Disease. The TrpV4 channelopathies are complex (3). A fundamental issue is whether the mutant channels have no-to-low (loss-of-function, LOF) or abnormally high (gain-of-function, GOF) activities. Even a complete loss of TrpV4 functions does not cause diseases because $trpV4^{-/-}$ knockout mice develop normally with only minor phenotypes (28, 29). Our results presented here and previously (5) show that diseases are likely all GOF effects, and by cytoplasmic Ca^{2+} poisoning. Small constitutive leakage may be manageable, but different alleles may respond to aggravating local and/or temporal stimuli differently, leading to disease variations. Reported electrophysiological results differ among laboratories. *TRPV4* is commonly expressed in cultured cells, producing subnA (10^{-10} to 10^{-9} Amp) whole-cell current. Whole *Xenopus* oocytes express μA (10^{-6} to 10^{-5} Amp) current (refs. 5, 14, and 30 and Fig. 4) and offer a much more favorable signal-to-noise ratio. Swelling activates TrpV4 in HEK cells (2, 3), though stretch activation, especially at the physiological temperature, has not been reported. Numerous intra- and intersubunit bonds maintain the closed state of a protein as complex as the TrpV4 tetramers. Therefore, there should be many ways to destabilize the closed state. The unusual findings here are that we have discovered one specific way of how the closed-state is destabilized and that the investigation revealed a normal, presumably physiological, disinhibition gating mechanism of TrpV4 by Ca^{2+}-CaM.

Methods

Wild-type or mutant *TRPV4* cRNAs were expressed in *Xenopus* oocytes, which were then examined with a two-electrode voltage clamp or a patch clamp in the excised inside-out mode. Calmodulin protein was presented to the patches directly from the bath. We also applied suctions on patches to examine channel mechanosensitivity. Detailed materials and methods are in SI Methods.

1. Garcia-Elias A, et al. (2014) The TRPV4 channel. *Handbook Exp Pharmacol* 222: 293–319.
2. Nilius B, Flockerzi V (2014) *Mammalian Trasient Receptor Potential (TRP) Cation Channels* (Springer-Verlag, Berlin).
3. Nilius B, Voets T (2013) The puzzle of TRPV4 channelopathies. *EMBO Rep* 14(2): 152–163.
4. Thorneloe KS, et al. (2008) N-((1S)-1-[4-((2S)-2-[(2,4-dichlorophenyl)sulfonyl]amino-3-hydroxypropanoyl)-1-piperazinyl]carbonyl-3-methylbutyl)-1-benzothiophene-2-carboxamide (GSK1016790A), a novel and potent transient receptor potential vanilloid 4 channel agonist induces urinary bladder contraction and hyperactivity: Part I. *J Pharmacol Exp Ther* 326(2):432–442.
5. Loukin S, Su Z, Kung C (2011) Increased basal activity is a key determinant in the severity of human skeletal dysplasia caused by TRPV4 mutations. *PLoS ONE* 6(5): e19533.
6. Rosenbaum T, Gordon-Shaag A, Munari M, Gordon SE (2004) Ca2+/calmodulin modulates TRPV1 activation by capsaicin. *J Gen Physiol* 123(1):53–62.
7. Gordon-Shaag A, Zagotta WN, Gordon SE (2008) Mechanism of Ca(2+)-dependent desensitization in TRP channels. *Channels (Austin)* 2(2):125–129.
8. Watanabe H, et al. (2003) Modulation of TRPV4 gating by intra- and extracellular Ca2+. *Cell Calcium* 33(5-6):489–495.
9. Strotmann R, Schultz G, Plant TD (2003) Ca2+-dependent potentiation of the non-selective cation channel TRPV4 is mediated by a C-terminal calmodulin binding site. *J Biol Chem* 278(29):26541–26549.
10. Strotmann R, Semtner M, Kepura F, Plant TD, Schöneberg T (2010) Interdomain interactions control Ca2+-dependent potentiation in the cation channel TRPV4. *PLoS ONE* 5(5):e10580.
11. Camacho N, et al. (2010) Dominant TRPV4 mutations in nonlethal and lethal metatropic dysplasia. *Am J Med Genet A* 152A(5):1169–1177.
12. Krakow D, et al. (2009) Mutations in the gene encoding the calcium-permeable ion channel TRPV4 produce spondylometaphyseal dysplasia, Kozlowski type and metatropic dysplasia. *Am J Hum Genet* 84(3):307–315.
13. Saimi Y, Ling KY (1990) Calmodulin activation of calcium-dependent sodium channels in excised membrane patches of Paramecium. *Science* 249(4975):1441–1444.
14. Loukin S, Zhou X, Su Z, Saimi Y, Kung C (2010) Wild-type and brachyolmia-causing mutant TRPV4 channels respond directly to stretch force. *J Biol Chem* 285(35): 27176–27181.
15. Trainees Of The Calcium Signals Laboratory EY, Yue DT (2015) Towards a unified theory of calmodulin regulation (calmodulation) of voltage-gated calcium and sodium channels. *Curr Mol Pharmacol*, in press.
16. Adelman JP (2015) SK channels and calmodulin. *Channels (Austin)*, in press.
17. Tidow H, et al. (2012) A bimodular mechanism of calcium control in eukaryotes. *Nature* 491(7424):468–472.
18. Ye Q, et al. (2013) Structural basis of calcineurin activation by calmodulin. *Cell Signal* 25(12):2661–2667.
19. Wahl-Schott C, et al. (2006) Switching off calcium-dependent inactivation in L-type calcium channels by an autoinhibitory domain. *Proc Natl Acad Sci USA* 103(42): 15657–15662.
20. Crump SM, Andres DA, Sievert G, Satin J (2013) The cardiac L-type calcium channel distal carboxy terminus autoinhibition is regulated by calcium. *Am J Physiol Heart Circ Physiol* 304(3):H455–H464.
21. Garcia-Elias A, et al. (2013) Phosphatidylinositol-4,5-biphosphate-dependent rearrangement of TRPV4 cytosolic tails enables channel activation by physiological stimuli. *Proc Natl Acad Sci USA* 110(23):9553–9558.
22. Dai J, et al. (2010) Novel and recurrent TRPV4 mutations and their association with distinct phenotypes within the TRPV4 dysplasia family. *J Med Genet* 47(10):704–709.
23. Liao M, Cao E, Julius D, Cheng Y (2013) Structure of the TRPV1 ion channel determined by electron cryo-microscopy. *Nature* 504(7478):107–112.
24. Numazaki M, et al. (2003) Structural determinant of TRPV1 desensitization interacts with calmodulin. *Proc Natl Acad Sci USA* 100(13):8002–8006.
25. Lau SY, Procko E, Gaudet R (2012) Distinct properties of Ca2+-calmodulin binding to N- and C-terminal regulatory regions of the TRPV1 channel. *J Gen Physiol* 140(5): 541–555.
26. Maroto R, et al. (2005) TRPC1 forms the stretch-activated cation channel in vertebrate cells. *Nat Cell Biol* 7(2):179–185.
27. Oron Y, Dascal N (1992) Regulation of intracellular calcium activity in Xenopus oocytes. *Methods Enzymol* 207:381–390.
28. Suzuki M, Mizuno A, Kodaira K, Imai M (2003) Impaired pressure sensation in mice lacking TRPV4. *J Biol Chem* 278(25):22664–22668.
29. Tabuchi K, Suzuki M, Mizuno A, Hara A (2005) Hearing impairment in TRPV4 knockout mice. *Neurosci Lett* 382(3):304–308.
30. Loukin S, Su Z, Zhou X, Kung C (2010) Forward genetic analysis reveals multiple gating mechanisms of TRPV4. *J Biol Chem* 285(26):19884–19890.

MEDICAL SCIENCES